Was There a Basis for Anticipating the 2010 Russian Heat Wave?

Randall Dole[1], Martin Hoerling[1], Judith Perlwitz[2], Jon Eischeid[2], Philip Pegion[2], Tao Zhang[2], Xiao-Wei Quan[2], Taiyi Xu[2], and Donald Murray[2].

[1]NOAA/Earth System Research Laboratory, Physical Sciences Division, Boulder, Colorado, USA
[2]Cooperative Institute for Research in Environmental Sciences, University of Colorado, Boulder, Colorado, USA

Abstract:

The 2010 summer heat wave in western Russia was extraordinary, with the region experiencing the warmest July since at least 1880 and numerous locations setting all-time maximum temperature records. This study explores whether early warning could have been provided through knowledge of natural and human-caused climate forcings. Model simulations and observational data are used to determine the impact of observed sea surface temperatures (SSTs), sea ice conditions and greenhouse gas concentrations. Analysis of forced model simulations indicates that neither human influences nor other slowly evolving ocean boundary conditions contributed substantially to the magnitude of this heat wave. They also provide evidence that such an intense event could be produced through natural variability alone. Analysis of observations indicate that this heat wave was mainly due to internal atmospheric dynamical processes that produced and maintained a strong and long-lived blocking event, and that similar atmospheric patterns have occurred with prior heat waves in this region. We conclude that the intense 2010 Russian heat wave was mainly due to natural internal atmospheric variability. Slowly varying boundary conditions that could have provided predictability and the potential for early warning did not appear to play an appreciable role in this event.

1. Introduction

Questions of vital societal interest are whether the 2010 Russian heat wave might have been anticipated, and to what extent human-caused greenhouse gas emissions played a role. Exceptional heat and poor air quality due to wildfires led to large increases in deaths in Moscow and elsewhere in western Russia, despite international efforts to improve public health responses to heat waves [*World Health Organization,* 2009]. Russia's extreme heat commenced in July nearly coincident with the peak temperatures in the annual cycle, thereby exacerbating human and environmental impacts. During July, when daily temperatures (Figure 1, top) were consistently near or above record levels, the heat wave spanned western Russia, Belarus, the Ukraine, and the Baltic nations (see Figure S1 in auxiliary material). Despite record warm globally-averaged surface temperatures over the first six months of 2010 [*National Climatic Data Center,* 2010], Moscow experienced an unusually cold winter and a relatively mild but variable spring, providing no hint of the record heat yet to come (Figure 1, top).

For the 2003 western European heat wave, human influences are estimated to have at least doubled the risk for such an extreme event [*Stott et al.,* 2004]. Other boundary forcings also contributed to the 2003 European heat wave, including anomalous sea surface temperatures (SSTs) [*Feudale and Shukla,* 2010]. The goal of this study is to identify the primary causes of the Russian heat wave and to assess to what it extent it might have been anticipated from prior knowledge of natural and human forcings and observed regional climate trends.

2. Data and model experiments

Our primary surface temperature data set is the National Oceanic and Atmospheric Administration (NOAA) Land/Sea Merged analyses [*Smith and Reynolds*, 2005]. Results derived from this data set are compared with those obtained from three other observational temperature data sets (see Table S1 and references for these data sets in the auxiliary material). In the following analyses, western Russia temperatures are defined as area-averages over the region 50^{o}N-60^{o}N and 35^{o}E to 55^{o}E, the region of highest heat wave intensity and approximately centered over Moscow.

Model simulations were performed to determine the potential for anticipating the Russian heat wave. First, the potential influence of increasing greenhouse gas concentrations, aerosols, and other natural external forcings on western Russian temperatures was assessed from simulations of 22 CMIP3 models [*Meehl et al.,* 2007]. These models are forced by specified monthly variations in greenhouse gases and tropospheric sulphate aerosols for 1880-1999, and with the IPCC Special Emissions Scenario (SRES) A1B thereafter. About half of the models also include changes in solar radiance and the effects of volcanic eruptions for the period 1880-1999. Model time series of western Russian temperatures were normalized relative to the observed mean standard deviation for July from 1880 to 2009 so that the magnitude of interannual variability in all models was comparable with observed variability. Second, possible effects of specific boundary conditions observed during July 2010 period were evaluated. For this purpose, 50-member ensemble simulations were performed for each of two atmospheric general circulation models, the GFDL AM2.1 [*Delworth et al.,* 2006] and the middle atmosphere configuration of ECHAM5 (MAECHAM5) [*Roeckner et al.,* 2003], using observed global SST, sea ice and atmospheric carbon dioxide concentrations for July 2010. Responses to 2010 forcings were determined through comparisons with two parallel 50-member control simulations that used 1971-2000 mean climatological forcings. Third, predictions generated in June 2010 with NOAA's climate forecast system model [*Saha et al*., 2006] were examined to assess the potential role of atmospheric and ocean initial conditions in this event. These predictions were initialized with atmosphere and ocean conditions in early (1-4) and late (27-30) June 2010.

3. Results

The July surface temperatures for the region impacted by the 2010 Russian heat wave shows no significant warming trend over the prior 130-year period from 1880 to 2009 (Fig. 1, middle and bottom). A linear trend calculation yields a total temperature change over the 130 years of -0.1^{o}C (with a range of 0 to -0.4^{o}C over the four data sets, see Tables S1 and S2 in auxiliary material for comparison). Similarly, no significant difference exists between July temperatures over western Russia averaged for the last 65 years (1945-2009) versus the prior 65 years (1880-1944) (Table S2). There is also no clear indication of a trend toward increasing warm extremes. The prior 10 warmest Julys are distributed across the entire period and exhibit only modest clustering earlier in this decade, in the 1980s and in the 1930s (Fig. 1, middle panel). This behavior differs substantially from globally averaged annual temperatures, for which eleven of the last twelve years ending in 2006 rank among the twelve warmest years in the instrumental record since 1850 [*Intergovernmental Panel on Climate Change,* 2007]. The absence of prior July warming also differs from antecedent conditions for the 2003 western European heat wave, where a strong regional warming trend was detected over the twentieth century (see long-term trend map in Fig. 1, bottom), a significant fraction of which has been attributed to anthropogenic forcing [*Fischer and Schär,* 2010].

With no significant long-term trend in western Russia July surface temperatures detected over the period 1880-2009, mean regional temperature changes are thus very unlikely to have contributed substantially to the magnitude of the 2010 Russian heat wave. Another possibility is that long-term trends *in variability* may have increased the likelihood of an extreme heat wave. To assess this possibility, standard deviations of July surface temperatures were calculated for the two 65-yr periods before and after 1945. The results (Table S2) indicate slightly higher variability in the later period, but this increase is not statistically significant based on a standard F-test. Western Russia temperature extremes simulated in the 22 CMIP3 models (grey shaded area in Figure 1, middle) also do not display discernible trends during 1880-2009. The temporal distribution of extreme heat waves in the model data normalized to correspond with observed variability shows two events of similar magnitude to the heat wave intensity of about +5°C departure observed during 1880-2009, with one event in the earlier half of the 20th Century (light gray shading in Fig. 1, middle). For model runs that are not normalized, the frequency of >5^{o}C extreme events occurring before 1945 is even greater and comparable in frequency to that seen in more recent decades (dark gray shading in Fig. 1 middle). In summary, the analysis of the observed 1880-2009 time series shows that no statistically significant long-term change is detected in either the mean or variability of western Russia July temperatures, implying that for this region an anthropogenic climate change signal has yet to emerge above the natural background variability. This is in contrast to regions such as western Europe, but similar to other regions like the central United States, consistent with strong regional (and seasonal) differences in climate trends that are yet to be fully understood.

The nature of this heat wave and its origins were intimately tied to the upper-level atmospheric flow. The 500 hPa July flow (Fig. 2, top) was characterized by a classic “omega” blocking pattern [*Dole and Gordon*, 1983]. The highest July 2010 surface temperature anomalies (Fig. 2, second panel) occurred near the center of the block, where northward displaced subtropical air, descending air motions and reduced cloudiness all contributed to abnormally warm surface temperatures. Severe drought occurred with the Russian heat wave, making it likely that land surface feedbacks amplified this heat wave’s intensity, as has been observed in prior severe droughts [*Atlas et al.,* 1993; *Fischer et al*., 2007]. To the east of the heat wave region, anomalously cool temperatures occurred in conjunction with an upper level trough and southward transport of polar air.

Russia is climatologically disposed toward blocking events during summer [*Tyrlis et al.,* 2007], and many of its prior July heat waves were associated with blocks. Consistent with this, a composite analysis of the average temperature anomalies and 500 hPa heights associated with the ten largest prior heat waves in this region since 1880 shows patterns similar to 2010 (cf. top two and bottom two panels in Figure 2), although features are weaker as expected from such an analysis. The distance between centers of the temperature anomalies is comparable to the scale for stationary upper-air Rossby waves [*Held et al.*, 1983], consistent with the role of atmospheric dynamical processes in accounting for the persistence of this pattern.

We have diagnosed additional model simulations forced by observed boundary conditions for this period to assess whether those may have produced a forced response consistent with the blocking pattern and associated heat wave. These boundary conditions reflect a mixture of both natural and human influences on the climate system. The observed global SSTs include positive anomalies in the Indo-west Pacific Ocean and tropical Atlantic and developing La Niña conditions in the east Pacific (see Fig. S1). The observed Arctic sea ice extent in July 2010 was the second lowest in the satellite record [*National Snow and Ice Data Center,* 2010]. Figure 3 shows the model response based on the AM2.1 model. The ensemble-mean responses of the atmospheric circulation (Fig. 3, top) and surface temperatures (Figure 3, second panel) are far weaker and their patterns are inconsistent with the observed blocking and heat wave (cf. Figure 2). A similar conclusion is drawn from the MAECHAM5 simulation whose response to July 2010 forcing is also very weak (Figure S2 in auxiliary material). These findings suggest that the blocking and heat wave were not primarily a forced response to specific boundary conditions during 2010.

Nor are there indications that blocking would increase in response to increasing greenhouse gases. Results using very high-resolution climate models suggest that the number of Euro-Atlantic blocking events will decrease by the latter half of the 21st century [*Matsueda et al.,* 2009; *Matsueda and Palmer, personal communication,* 2010]. The horizontal resolution of climate models is an important consideration in simulating blocking accurately. Although the ensemble-mean AM2.1 and MAECHAM5 responses bear no resemblance to the observed event, both models are capable of producing blocking over this area. For example, individual members within each model ensemble show flow patterns (Figures 3 and S2, third panels) and temperature anomalies (Figures 3 and S2, bottom panels) that are qualitatively similar to observations. However, these patterns reflect internal atmospheric variability within the models rather than a systematic response to boundary forcing, and thus are not evidence of a predictable signal. With only 50 ensemble members in these simulations, a meaningful assessment of changes in the tails of the distributions is not possible.

A third suite of model runs has also been considered which differs from the prior sets in that it is initialized with observed ocean-atmosphere-land conditions of 2010 in NOAA's operational coupled Climate Forecast System (CFS). Comparing predictions of July blocking in models initialized in early June versus in late June further clarifies the roles of boundary forcing and initial conditions and also addresses the potential for early warning capabilities. When initialized in early June 2010, the predictions show no evidence for a change in the probability of prolonged daily blocking during July 2010 over western Russia compared to the July hindcasts that were initialized in each June during 1981-2008. The model predictions do, however, show approximately a doubling of the average duration of daily blocking during July for runs begun in late June, by which time blocking was already present in atmospheric initial conditions (see Figure S3 in the auxiliary material). This increase coincides with a shift of the probability density function of western Russian temperature anomalies towards warmer values by about +1.5^{o}C. These results are consistent with the interpretation that the Russian heat wave was primarily caused by internal atmospheric dynamical processes rather than observed ocean or sea ice states or greenhouse gas concentrations.

4. Concluding remarks

Our analysis points to a primarily natural cause for the Russian heat wave. This event appears to be mainly due to internal atmospheric dynamical processes that produced and maintained an intense and long-lived blocking event. Results from prior studies suggest that it is likely that the intensity of the heat wave was further increased by regional land surface feedbacks. The absence of long-term trends in regional mean temperatures and variability together with the model results indicate that it is very unlikely that warming attributable to increasing greenhouse gas concentrations contributed substantially to the magnitude of this heat wave. Nevertheless, there is evidence that such warming has contributed to observed heat waves in other regions, and is very likely to produce more frequent and extreme heat waves later this century [*Intergovernmental Panel on Climate Change,* 2007]. To assess this possibility for the region of western Russia, we have used the same IPCC model simulations to estimate the probability of exceeding various July temperature thresholds over the period 1880-2100 (Figure 4). The results suggest that we may be on the cusp of a period in which the probability of such events increases rapidly, due primarily to the influence of projected increases in greenhouse gas concentrations. Uncertainty in timing is nonetheless evident (Fig. 4, inset), due in part to different model sensitivities to greenhouse gas forcing. Understanding the physical processes producing heat waves will be important for improving regional projections, and may also provide an improved capability for predicting some extreme events. However, as in the case of the 2010 Russian heat wave, events will also occur that are not readily anticipated from knowledge of either prior climate trends or specific climate forcings, and for which advance warning may thus be limited.

Acknowledgements The study is supported in part by the NOAA Climate Program Office. The CFS forecast data were provided by Dr. Wanqui Wang of NOAA's Climate Prediction Center. The comments provided by Drs. William Neff and Klaus Wolter are gratefully acknowledged.

References

Atlas, R., N. Wolfson, and J. Terry (1993), The effects of SST and soil moisture anomalies on GLA model simulations of the 1988 US summer drought. *J. Climate, 6,* 2034-2048.

Compo, G. P. et al. (2009), The Twentieth Century Reanalysis Project. *Quarterly J. Roy. Met. Soc.*, doi: 10.1002/qj.776.

Delworth, T. L. et al. (2006), GFDL's CM2 Global Coupled Climate Models. Part I: Formulation and simulation characteristics. *J. Climate*, *19*, 643-674.

Dole, R. M., and N. D. Gordon (1983), Persistent anomalies of the extra-tropical Northern Hemisphere wintertime circulation: Geographical distribution and regional persistence characteristics. *Mon. Wea. Rev*., *111*, 1567–1586.

Feudale, L., and J. Shukla (2010), Influence of sea surface temperature on the European heat wave of 2003 summer. Part II: a modeling study. *Clim. Dyn.*, doi 10.1007/s00382-010-0789-z.

Fischer, E. M., and C. Schär (2010), Consistent geographical patterns of changes in high-impact European heatwaves. *Nature Geo*., doi:10.1038/NGEO866.

Intergovernmental Panel on Climate Change (2007), Climate Change 2007: The Physical Science Basis. Contribution of Working Group I to the Fourth Assessment Report of the Intergovernmental Panel on Climate Change, edited by S. Solomon et al., Cambridge Univ. Press, Cambridge, U. K.

Held, I. M. (1983), Stationary and quasi-stationary eddies in the extratropical troposphere. In *Large-scale Dynamical Processes in the Atmosphere,* B. Hoskins and R. Pearce Eds., 127-168

Meehl, G., et al. (2007), The WCRP CMIP3 multimodel dataset: A new era in climate change research, Bull. Am. Meteorol. Soc., 88, 1383–1394, doi:10.1175/BAMS-88-9-1383.

Matsueda, M., R. Mizuta, and S. Kusunoki (2009), Future change in wintertime atmospheric blocking simulated using a 20-km-mesh atmospheric global circulation model, *J. Geophys. Res.*, *114*, D12114, doi:10.1029/2009JD011919.

National Climatic Data Center (2010), State of the Climate: Global Analysis for June 2010, published online July 2010, http://www.ncdc.noaa.gov/sotc/?report=global&year=2010&month=6.

National Snow and Ice Data Center (2010) Arctic sea ice news and analysis, August 4 2010 http://nsidc.org/arcticseaicenews/2010/080410.html

Roeckner, E., and Coauthors, 2003: The atmospheric general circulation model ECHAM5. Part I. Model description. MPI Report 349, Max-Planck-Institut für Meteorologie, Hamburg, Germany, 127 pp.

Saha, S. et al. The NCEP Climate Forecast System. *J. Climate*, **19**, 3483-3517 (2006).

Schär, C., P.L. Vidale, D. Lüthi, C. Frei, C. Häberli, M. Liniger and C. Appenzeller, 2004: The role of increasing temperature variability in European summer heat waves. *Nature*, *427*, 332-336.

Smith, T. M., and R. W. Reynolds (2005), A global merged land air and sea surface temperature reconstruction based on historical observations (1880–1997), J. Clim., 18, 2021–2036, doi:10.1175/JCLI3362.1.

Stott, P. A., D. A. Stone, and M. R. Allen (2004). Human contribution to the European heat wave of 2003. *Nature 432,* 610-614.

Tyrlis, E., and B.J. Hoskins (2007), Aspects of a Northern Hemisphere atmospheric blocking climatology. *J. Atmos. Sci*, **65**, doi: 10.1175/2007JAS2337.1.

World Health Organization, (2009), Improving public health responses to extreme weather/heat waves- EuroHEAT. B. Menne and F. Matthies, Eds. WHO Regional Office for Europe, Copenhagen, Denmark. Technical summary (http://www.euro.who.int/__data/assets/pdf_file/0010/95914/E92474.pdf) 60 pp (2009).

Figure Captions

Figure 1: *Top panel:* Daily Moscow temperature record from November 1 2009 to October 31 2010, with daily departures computed with respect to the climatological seasonal cycle. Data are from the Global Summary of the Day produced by National Climatic Data Center.

Middle panel: Observed time series of western Russia July temperature anomalies for the period 1880 to 2010 indicated as positive (red) and negative (blue) temperature anomalies relative to the base period from 1880 to 2009. Numbers indicate the years of the ten most extreme positive anomalies. The red star indicates year 2010. The light and dark shaded areas represents the envelopes of positive and negative monthly mean temperature extremes based on 22 CMIP3 model simulations for normalized and non-normalized anomaly time series respectively

Bottom Panel: Map of observed July temperature trend [^{o}C/130yrs] for July 1880-2009. Box shows the area used to define "western Russia" surface temperatures.

Figure 2: Observed climate conditions for July 2010 and for the 10 warmest western Russia July temperatures since 1880.

Top panel: NCEP/NCAR Reanalysis 500 hPa height (contour, contour interval: 100 m), anomalies (shading), and wind vector anomalies (arrows, m s^{-1}) for July 2010. Anomalies are relative to the 1948-2009 climatology.

Second panel: Observed surface air temperature anomalies for July 2010 (base period is 1880-2009) from the NOAA merged land air and sea surface temperature dataset.

Third and bottom panels: As first and second panels but for composite of the ten warmest July monthly means over western Russia during the period 1880-2009. The Twentieth Century Reanalysis are the data source of 500 hPa heights [*Compo et al.,* 2011].

Figure 3: July 2010 climate conditions simulated with GFDL AM2.1

Top panel: The 50 member ensemble mean of 500 hPa height (contour, contour interval: 100 m), anomalies (shading), and wind vector anomalies (arrows).

Second panel: Ensemble-mean surface temperature anomalies.

Third and bottom panel: As in top and second panels, but for a single model run selected from the ensemble.

Figure 4: Simulated frequency of occurrence of western Russia temperature extremes for 30-year overlapping periods. Shown are time series for exceedance values of 3, 4, 5 and 6^{o}C. Values are calculated based on 22 CMIP3 model ensemble. Insert shows the time series for the number of models in [%] that simulate at least a 10% probability of occurrence of a heat wave with specific temperature exceedance values.

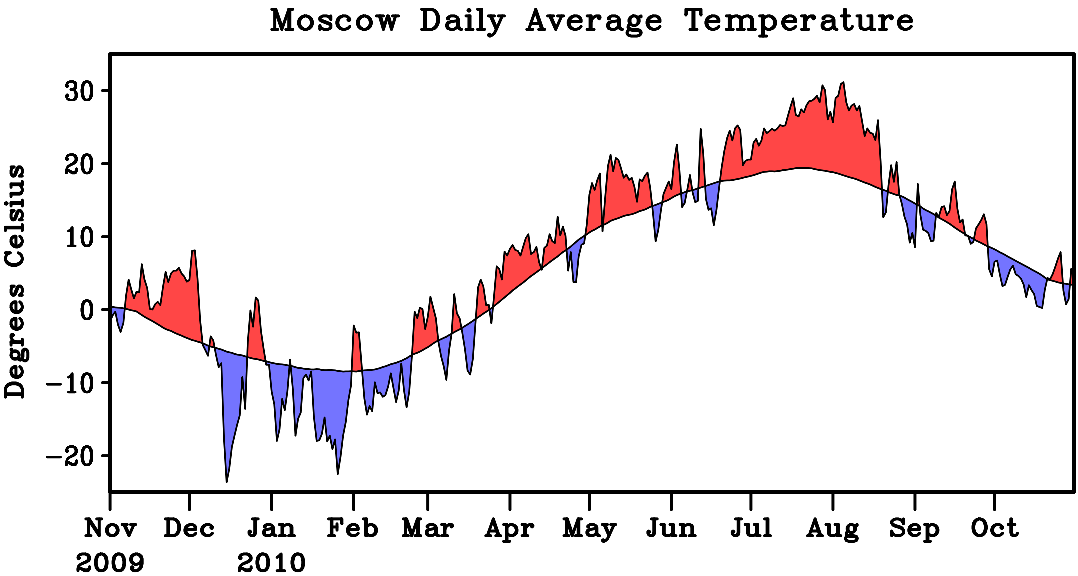
Moscow Daily Average Temperature
Degrees Celsius
30
20
10
0
−10
−20
Nov
2009
Dec
Jan
2010
Feb
Mar
Apr
May
Jun
Jul
Aug
Sep
Oct

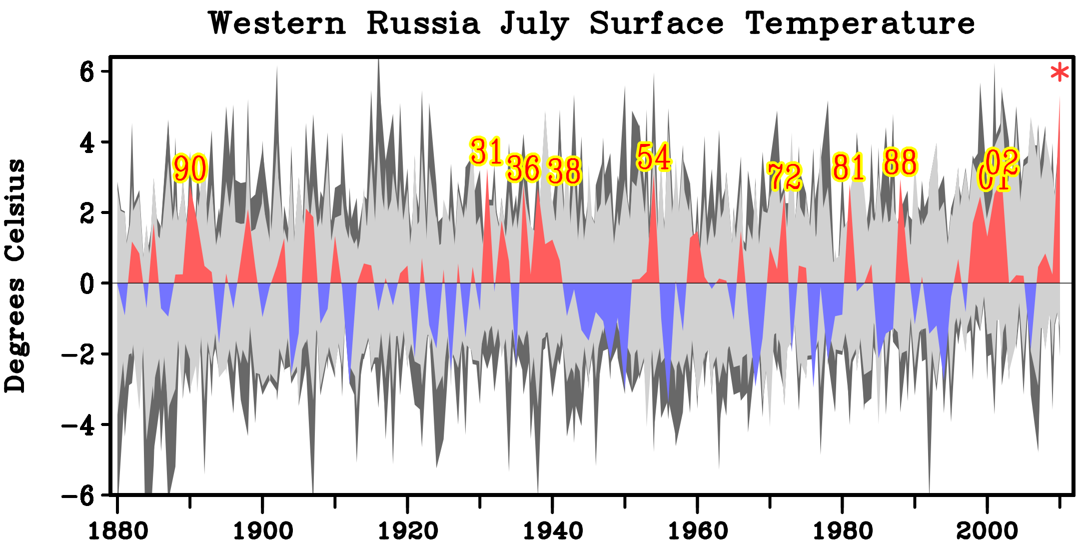
Western Russia July Surface Temperature
Degrees Celsius
6
4
2
0
−2
−4
−6
90
31
36
38
54
72
81
88
01
02
*
1880
1900
1920
1940
1960
1980
2000

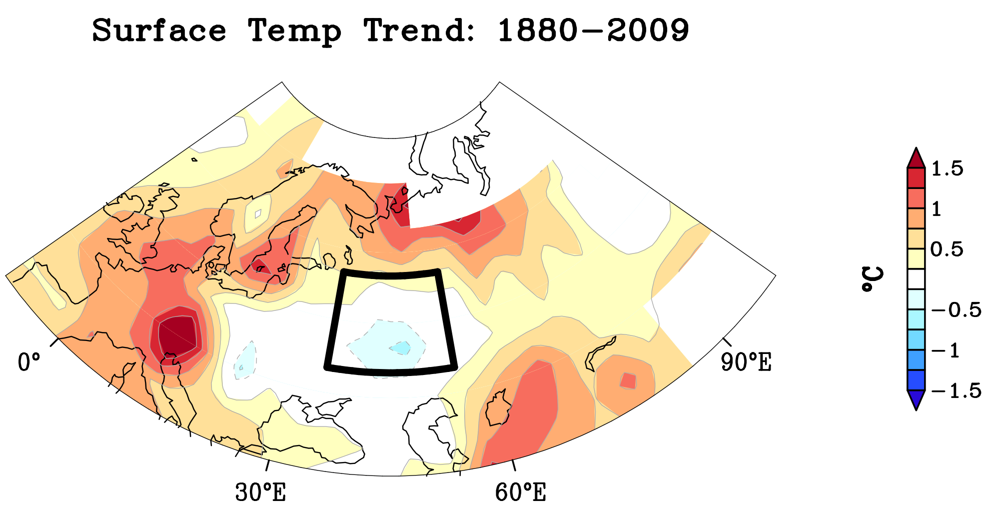
Surface Temp Trend: 1880−2009
0°
30°E
60°E
90°E
1.5
1
0.5
−0.5
−1
−1.5
°C

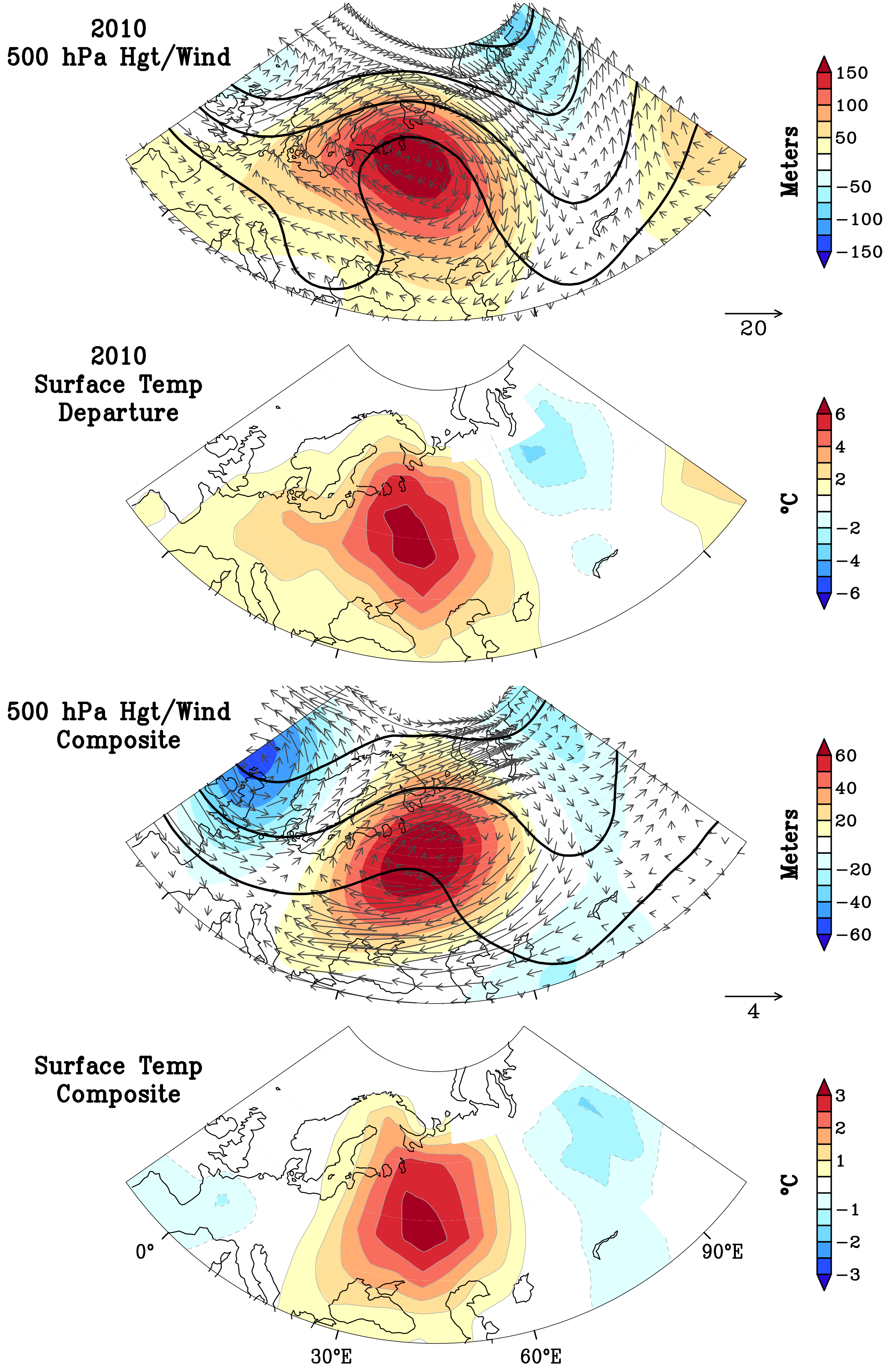

2010
500 hPa Hgt/Wind
150
100
50
-50
-100
-150
Meters
20
2010
Surface Temp
Departure
6
4
2
-2
-4
-6
°C
500 hPa Hgt/Wind
Composite
60
40
20
-20
-40
-60
Meters
4
Surface Temp
Composite
3
2
1
-1
-2
-3
°C
0°
90°E
30°E
60°E

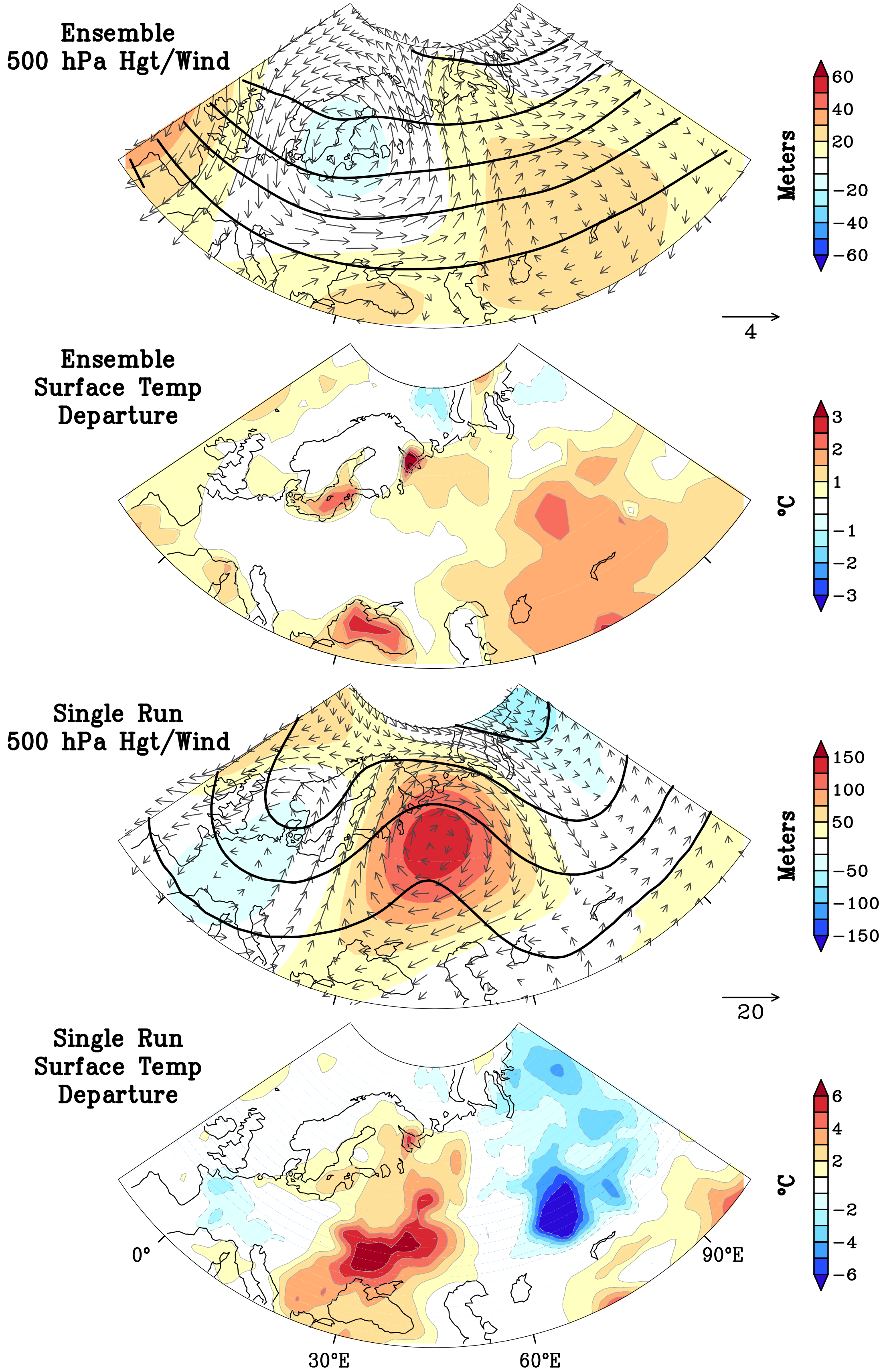
Ensemble
500 hPa Hgt/Wind
Meters
60
40
20
−20
−40
−60
4
Ensemble
Surface Temp
Departure
°C
3
2
1
−1
−2
−3
Single Run
500 hPa Hgt/Wind
Meters
150
100
50
−50
−100
−150
20
Single Run
Surface Temp
Departure
°C
6
4
2
−2
−4
−6
0°
30°E
60°E
90°E

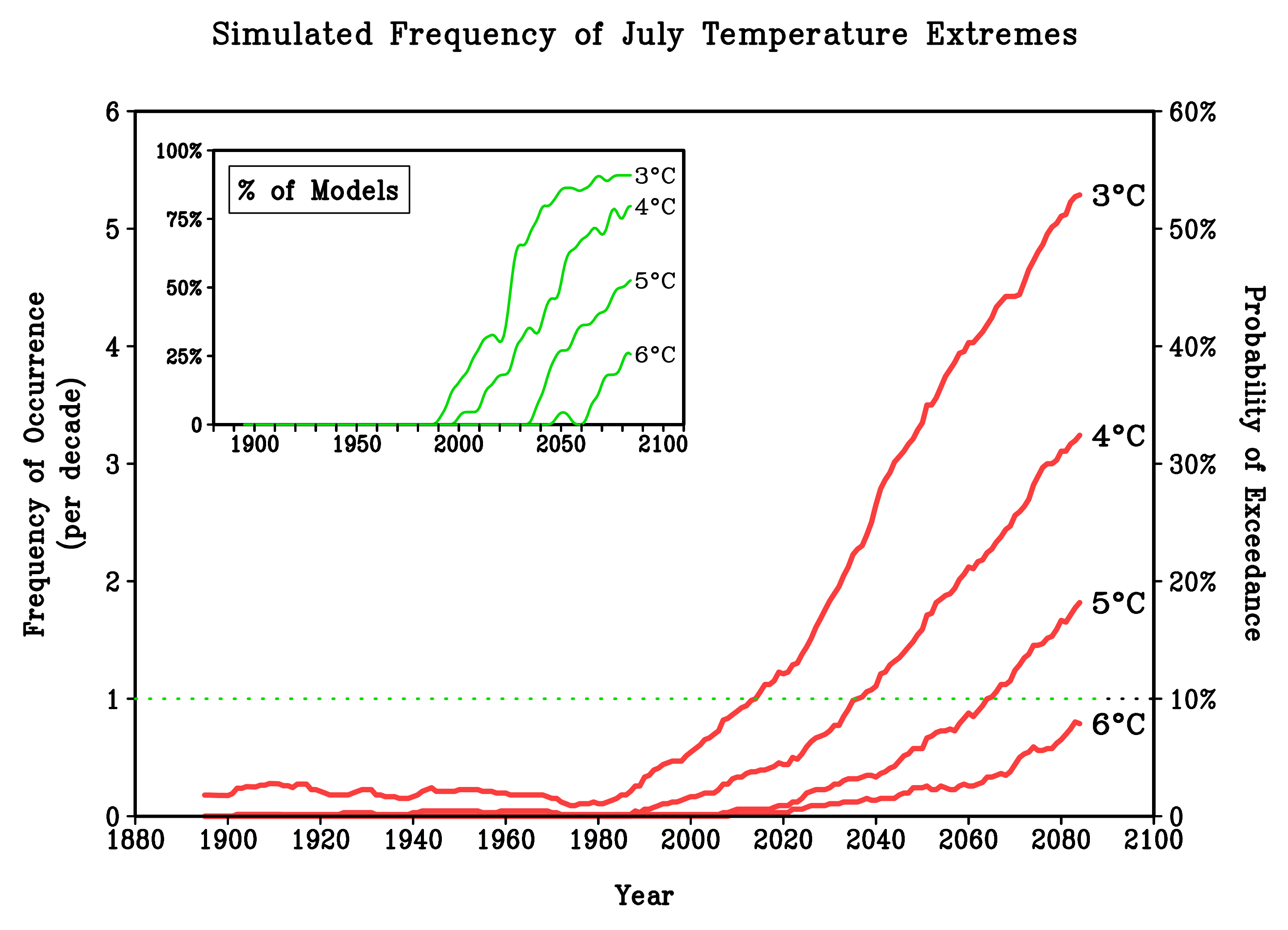
Simulated Frequency of July Temperature Extremes
% of Models
3°C
4°C
5°C
6°C
100%
75%
50%
25%
0
1900
1950
2000
2050
2100
Frequency of Occurrence (per decade)
Probability of Exceedance
Year
6
5
4
3
2
1
0
60%
50%
40%
30%
20%
10%
1880
1900
1920
1940
1960
1980
2000
2020
2040
2060
2080
2100

Auxiliary Material:

Was There a Basis for Anticipating the 2010 Russian Heat Wave?

Randall Dole, Martin Hoerling, Judith Perlwitz, Jon Eischeid, Philip Pegion, Tao Zhang, Xiao-Wei Quan, Taiyi Xu, and Donald Murray

A: Temperature statistics for western Russia based on four temperature data sets

Table S1: Temperature statistics for western Russia based on the following four temperature data sets: National Oceanic and Atmospheric Administration (NOAA) Land/Sea Merged Temperatures [*Smith and Reynolds,* 2005], NOAAs's National Climate Data Center (NCDC) Gridded Land Temperatures based on the Global Historical Climatology Network (GHCN) [*Peterson and Vose*, 1997]. U.K. Hadley Center's HadCRUT3v [*Brohan et al.,* 2006], National Aeronautics and Space Administration (NASA) Goddard Institute for Space Studies Surface Temperature Analysis (GISTEMP) [*Hansen et al.,* 2001]. Shown are temporal correlations with the NOAA data set for July time series, July 2010 values, and linear trend for the period 1880-2009.

Data Set	Correlation with NOAA Temperature	July 2010 value [ºC]	Linear Trend1880-2009 [ºC/130 years]
NOAA	1.0	5.3	-0.12
NCDC	0.97	4.8	0.03
HadCRUT3v	0.98	5.4	-0.41
GISTEMP	0.99	5.7	-0.33

Table S2: Comparison of mean anomalies and variance between the periods P1:1880-1944 and PII: 1945-2009 for western Russian temperature records based on four data sets described in Table S1. Anomalies are relative to the period 1880-2009. Absolute t-values larger |1.65| indicate that differences between the later and earlier period are statistically significant at least at the 95% level. F-values larger 1.53 indicate that the variances of the first and second period are significantly different at the 90% level.

Data set	**Mean [ºC]**			**Variance [ºC^2]**		
	PI	PII	t-value (PII – PI)	PI	PII	F-value (PII/PI)
NOAA	0.10	-0.18	-1.09	1.85	2.40	1.30
NCDC	0.01	-0.10	-0.60	1.04	1.23	1.18
HadCRUT3v	0.18	-0.26	-1.80	1.90	2.01	1.06
GISTEMP	0.15	-0.23	-1.49	1.99	2.25	1.13

B: Map of observed global temperature anomalies for July 2010

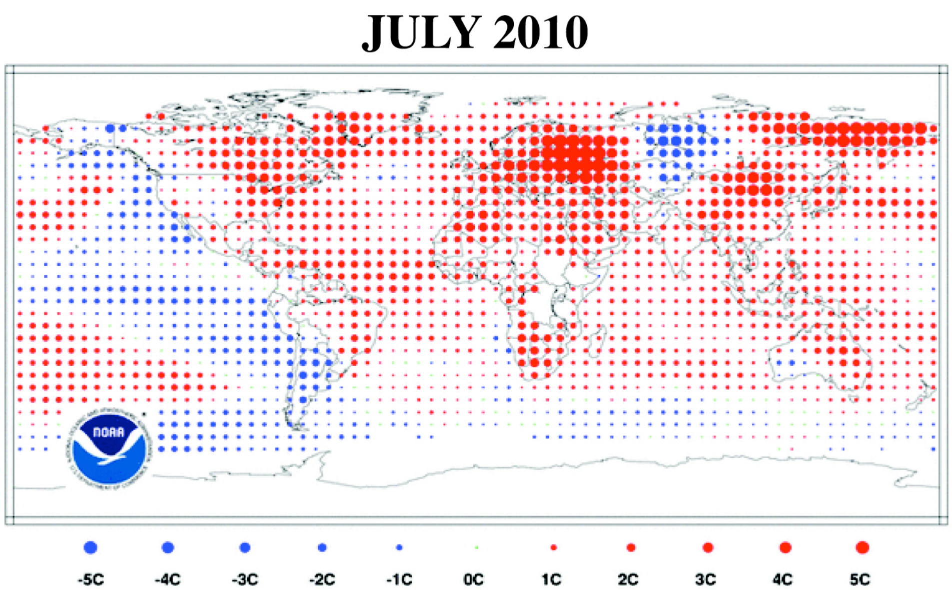

Figure S1: Map of observed global temperature anomalies for July 2010, from NOAA analyses produced by the National Climatic Data Center (NCDC). Anomalies are determined with respective to the base period 1971 to 2000.

C: July 2010 climate conditions simulated with MAECHAM5

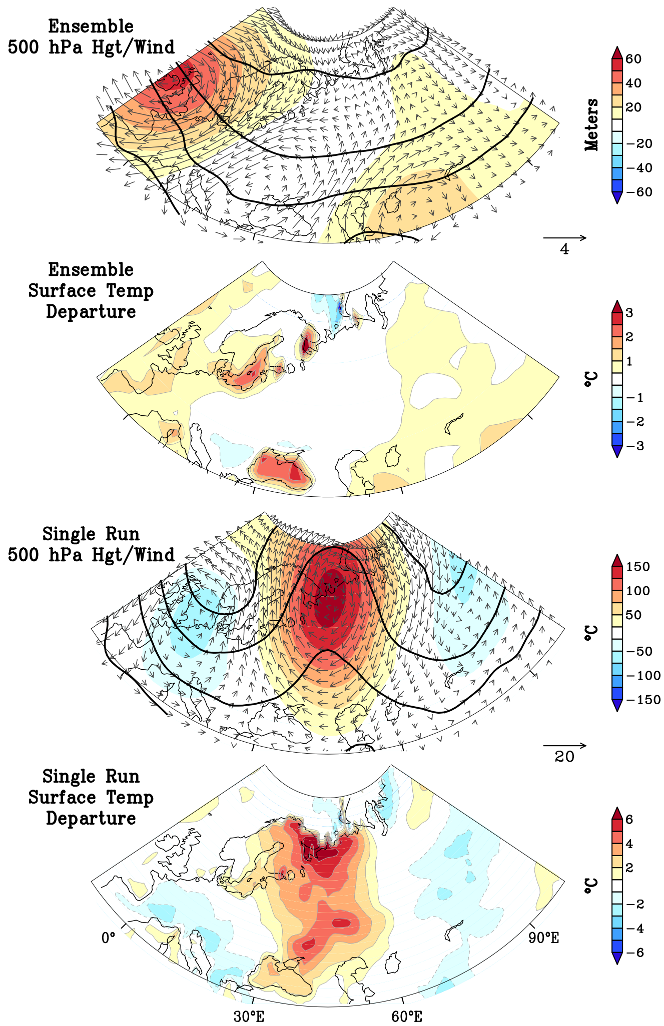

Figure S2: July 2010 climate conditions simulated with MAECHAM5
Top panel: The 50 member ensemble mean of 500 hPa height (contour, contour interval: 100 m), anomalies (shading), and wind vector anomalies (arrows, m s^{-1}).
Second panel: Ensemble mean surface temperature anomalies
Third and bottom panel: As in top and second panels, but for a single model run selected from the ensemble.

D: July blocking statistics in the NOAA Climate Forecast System and Reanalysis

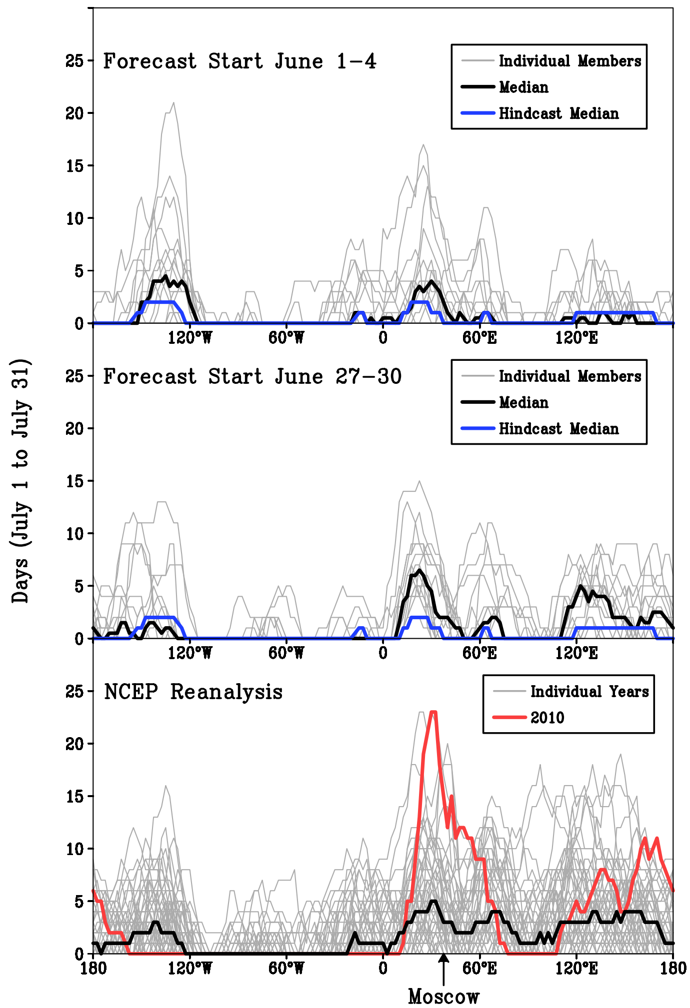

Figure S3: The number of blocking days during July between 55°N-65°N at all longitudes using the approach by *Tibaldi and Molteni* [1990].

Top panel: The number of blocking days from the NOAA Climate Forecast System (CFS) model 16-ensemble forecasts with initial conditions on June 1-4 2010 (thin black lines), and the median of 16 samples (thick black line). The thick blue line indicates the median value of the hindcast ensemble with June initial conditions (1981-2008).

Middle panel: Same as upper panel but for initial conditions on June 27-30 2010.

Bottom panel: Number of blocking days determined from NCEP/NCAR reanalysis for 1948-2009 (thin black lines), for 2010 (red line), and the median of 63 years (thick black line).

E: References for temperature data sets and additional diagnostics

Brohan, P., J. J. Kennedy, I. Harris, S. F. B. Tett, and P. D. Jones (2006), Uncertainty estimates in regional and global observed temperature changes: A new dataset from 1850, *J. Geophys. Res., 111,* D12106, doi:10.1029/2005JD006548.

Hansen, J., R. Ruedy, M. Sato, M. Imhoff, W. Lawrence, D. Easterling, T. Peterson, and T. Karl (2001), A closer look at United States and global surface temperature change, *J. Geophys. Res., 106*, 23,947–23,963, doi:10.1029/2001JD000354.

Peterson, T. C., and R. S. Vose (1997), An overview of the Global Historical Climatology Network temperature database, *Bull. Am. Meteorol. Soc., 78,* 2837–2849, doi:10.1175/1520-0477(1997)078<2837: AOOTGH>2.0.CO;2.

Smith, T. M., and R. W. Reynolds (2005), A global merged land air and sea surface temperature reconstruction based on historical observations (1880–1997), *J. Clim., 18*, 2021–2036, doi:10.1175/JCLI3362.1.

Tibaldi, S. and F. Molteni (1990), On the operational predictability of blocking. Tellus, 42A, 343-365.